

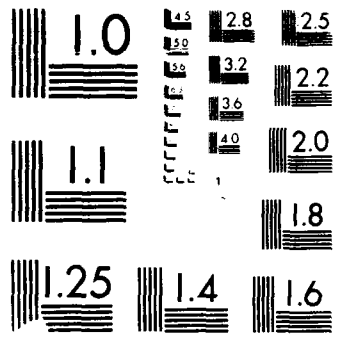
AD-A207 934 THE DESIGN OF A TE SUB 13 MODE PHASE LOCKED OSCILLATOR 1/1
(U) NAVAL RESEARCH LAB WASHINGTON DC J BURKE ET AL.
10 APR 89 NRL-MR-6434

UNCLASSIFIED

F/G 9/1

NL

ET NO
FILMED
6/89
DUC



al Research Laboratory

gton, DC 20375-5000



2

NRL Memorandum Report 6434

AD-A207 934

The Design of a TE_{13} Mode Phase Locked Oscillator

JOHN BURKE,* WALLACE MANHEIMER AND MARK CZARNASKI,**

*High Power Electromag Radiation Branch
Plasma Physics Division*

**Burke Technology, San Diego, CA*

***JAYCOR, McLean, VA*

DTIC
ELECTE
MAY 19 1989
S D

April 10, 1989

REPORT DOCUMENTATION PAGE				Form Approved OMB No 0704 0188	
1a REPORT SECURITY CLASSIFICATION UNCLASSIFIED		1b RESTRICTIVE MARKINGS			
2a SECURITY CLASSIFICATION AUTHORITY		3 DISTRIBUTION AVAILABILITY OF REPORT Approved for public release; distribution unlimited.			
2b DECLASSIFICATION/DOWNGRADING SCHEDULE					
4 PERFORMING ORGANIZATION REPORT NUMBER(S) NRL Memorandum Report 6434		5 MONITORING ORGANIZATION REPORT NUMBER(S)			
6a NAME OF PERFORMING ORGANIZATION Naval Research Laboratory	6b OFFICE SYMBOL (if applicable) Code 4740	7a NAME OF MONITORING ORGANIZATION			
6c ADDRESS (City, State, and ZIP Code) Washington, DC 20375-5000		7b ADDRESS (City, State, and ZIP Code)			
8a NAME OF FUNDING SPONSORING ORGANIZATION SDIO/ONR	8b OFFICE SYMBOL (if applicable)	9 PROCUREMENT INSTRUMENT IDENTIFICATION NUMBER			
8c ADDRESS (City, State, and ZIP Code) Washington, DC		10 SOURCE OF FUNDING NUMBERS			
		PROGRAM ELEMENT NO	PROJECT NO	TASK NO	WORK UNIT ACCESSION NO
11 TITLE (Include Security Classification) The Design of a TE ₁₃ Mode Phase Locked Oscillator					
12 PERSONAL AUTHOR(S) Burke,* J., Manheimer, W. and Czarnaski,** M.					
13a TYPE OF REPORT	13b TIME COVERED FROM 10/86 TO 10/87	14 DATE OF REPORT (Year, Month, Day) 1989 April 10	15 PAGE COUNT 48		
16 SUPPLEMENTARY NOTATION *Burke Technology, San Diego, CA **JAYCOR, McLean, VA					
17 COSATI CODES		18 SUBJECT TERMS (Continue on reverse if necessary and identify by block number)			
FIELD	GROUP	SUB GROUP	Phase locked oscillator.		
			Gyrotron		
			Gyroklystron		
19 ABSTRACT (Continue on reverse if necessary and identify by block number)					
<p>The design is presented of a TE₁₃ Mode Phase Locked Gyrotron Oscillator. The oscillator is phase locked by a signal injected into a prebunching cavity. As one extrapolates microwave tube technology to higher power and/or higher frequency, one is ultimately forced to deal with overmoded systems. The design trade-offs are constrained by the overmoded nature of both the oscillator and bunching cavity.</p>					
20 DISTRIBUTION AVAILABILITY OF ABSTRACT <input checked="" type="checkbox"/> UNANNOUNCED <input type="checkbox"/> SAVE AS PREP <input type="checkbox"/> OTHER USERS		21 ABSTRACT SECURITY CLASSIFICATION UNCLASSIFIED			
22a NAME OF PERSONS RESPONSIBLE FOR ABSTRACT Wallace M. Manheimer		22b TELEPHONE (Include Area Code) (202) 767-3128	22c MAILING ADDRESS Code 4740		

CONTENTS

I.	INTRODUCTION	1
II.	THE EXPERIMENTAL DESIGN	2
	REFERENCES	16
IV.	FEBETRON-GYROTRON SLOTTED CAVITY EXPERIMENTS	17
	DISTRIBUTION LIST	37

Accession For	
NTIS CRA&I	<input checked="" type="checkbox"/>
DTIC TAB	<input type="checkbox"/>
Unannounced	<input type="checkbox"/>
Justification	
By	
Distribution/	
Availability Codes	
Dist	Avail and/or Special
A-1	



THE DESIGN OF A TE_{13} MODE PHASE LOCKED OSCILLATOR

I. Introduction

The goal of the low power experiment is to study a phase-locked oscillator in the actual mode at which the high power phase-locked oscillator will run. The phase locking signal will be injected into an input cavity where it will prebunch the beam. The use of a prebunching cavity allows for amplification of the prebunching signal from the first to second cavity. Follow on designs which utilize additional buncher cavities allow for more amplification of the input signal. The mode of operation will be the TE_{13} mode in both the main cavity and in the prebunching cavity. A TE_{13} mode is about as overmoded as seems prudent to operate in a first experiment. Also, a very difficult problem in the design of the experiment is the stabilization of the prebunching cavity. The use of axial slots greatly reduces the cavity Q of all modes but the TE_{1n} modes. Furthermore, a TE_{1n} mode has the additional advantage that it is relatively simple to convert to a fundamental TE_{11} mode which is then quite easy to radiate. This experiment is designed using a thermionic electron beam and will be operable at high rep rate and high average power. The conceptual design of the 85 GHz two cavity phase locked oscillator is shown in Fig 1.

II The Experimental Design

The design is very complicated because both the oscillator and prebunching cavity have had to operate in a very overmoded configuration. Recently, it has been shown that with careful design, a high power free running gyrotron oscillator can operate in a single very high order mode.^{1,2} However, operation as a phase-locked oscillator puts many more constraints on the design than does operation as a free running oscillator. In addition to selecting the proper mode in the oscillator cavity, the phase-locked oscillator must be designed so as to suppress oscillation in the input cavity, launch the proper mode in the input cavity, and suppress communication between the input and oscillator cavities. Furthermore, the length of the drift section between the two cavities is limited by the thermal spread on the beam, as discussed in the previous section and elsewhere.³ For instance, it might be thought that one could always stabilize the prebunching cavity simply by making it short enough. However, if one uses sudden changes in the cavity radius to define the cavity, one can make the cavity very short, but one will have a great deal of mode conversion at the cavity edges. This mode conversion will both lower the Q of the input cavity and also effectively trap any radiation which leaks out of the main oscillator cavity. Alternatively, one could use

gentle tapers to define the cavity. This is, in fact, necessary to minimize mode conversion and our design does incorporate gentle tapers, and so will the gigawatt design. However, now one has fringe fields which extend far into the taper region, so that the effective cavity length is not simply the length of the straight section between the tapers, but is much longer. Even for zero straight section length, the effective length of the prebunching cavity can be considerable.

The longer one makes the taper on the cavity wall, the less mode conversion there will be. However, the taper cannot be made arbitrarily long either. For one thing, this makes the effective length of the prebunching cavity very long, and thereby more difficult to stabilize. Also, a long taper means a long drift section, so that thermal spread on the beam would greatly reduce the phase locking bandwidth. Thus, before the experiment can be set up, it is clear that a very careful, time consuming design is required.

Certain basic principles have become clear as we have proceeded with this design. First of all, our original strategy was to maximize the phase locking bandwidth by maximizing the field in the input cavity. This implied using a fairly high Q cavity for the input, and our original design choice was for a Q of five to ten thousand, not much less than the Ohmic Q . It was

expected that the input cavity would have a lower start oscillation current, but that the input cavity would be stable because the magnetic field would be too high for it to oscillate. That is the input cavity would be very short, so that above a critical field B_c it would be stable. The main cavity would be longer and would oscillate at higher fields. The start oscillation current for the input cavity and the main cavity as a function of the magnetic field, for our original design, is shown schematically in Fig. 2. One disadvantage of such design is immediately apparent. On the I-B parameter space of a single cavity gyrotron, the regime of most efficient operation is shown in Fig. 3. Clearly, the high Q input cavity does not allow the main cavity to access the regime of most efficient operation. Furthermore, one is in danger of having the input cavity self oscillate due to operating in magnetic fields which are slightly incorrect. Finally it was realized that even though the inherent bandwidth of the oscillator is larger, it is still limited by the low bandwidth of the input cavity.

For all of these reasons, the design was switched to a low Q input cavity design with less inherent locking bandwidth. The I-B parameter space of the phase-locked oscillator with the low Q input cavity is shown schematically in Fig. 4. The operating regime now encompasses the regime of most efficient operation,

and furthermore, there is no danger of the input cavity self oscillating at any magnetic field. While the inherent bandwidth is reduced, it also seems clear, in principle at least, that it can be increased by going to a multi-input-cavity configuration. By injecting the power in the first input cavity, one achieves amplification, so that the field in the second cavity is greater. This amplified field then prebunches the beam for the final oscillator cavity.

The total number of cavities is not limited by the thermal spread on beam; thermal spread on the beam only limits the intercavity spacing. At each intermediate cavity, an amplified field prebunches the beam at higher bunching parameter, so that on exiting one intermediate cavity, the beam effectively has no memory of the bunching in the cavities before. What does limit the number of cavities however is mode conversion. In the oscillator cavity, there is some mode conversion from, for instance, the $TE_{1,3}$ to the $TE_{1,2}$. This $TE_{1,2}$ mode propagates freely through the drift tube and through all of the prebunching cavities. As it passes each prebunching cavity, some of it is reconverted to the $TE_{1,3}$ in the prebunching cavity and is then trapped there. If all prebunching cavities are identical, the same fraction of the leaked out mode is trapped in all prebunching cavities. Specifically, some will be trapped in the first cavity. As long as the power trapped in the first cavity

is significantly less than the injected power, it should work as a multicavity phase-locked oscillator. Once the trapped power becomes comparable to the injected power, phase-locked operation clearly becomes nonviable. Thus, in an overmoded phase-locked oscillator, the mode conversion at the cavity tapers limits the number of prebunching cavities. This is in contrast to a fundamental mode oscillator or amplifier where there is no such limitation. For instance, the SLAC klystron has seven cavities altogether. It is unlikely that a $TE_{1,1}$ phase-locked oscillator could ever have nearly that many. However, it could probably have three, and this would be a potential follow on project to this if there is interest in enhancing the locking bandwidth.

The parameters of the low power oscillator are a frequency of 85 GHz, the operating mode is a $TE_{1,1}$ standing mode, the beam voltage is 70 kV, the current is 6 Amps or less, the output cavity Q is about 2000, the input cavity Q is about 1000, the isolation between the cavities is about 45 dB, the input power, from a Varian 85 GHz EIO is 500-1000 watts, and the output power will be 50-100 kW. The performance of the low power phase-locked oscillator has been examined using both the analytic theory for a $TE_{1,1}$ standing mode, and also the slow time scale theory for a $TE_{1,1}$ rotating mode. The analytic theory gives the result that

$$\frac{\Delta\omega}{\omega} = \frac{0.17 I(\text{Amps})}{E(\text{kV/cm})} (U^2 + V^2)^{1/2}$$

where E is the field in the oscillator cavity. Taking I=4 and E=250, we find that

$$\frac{\Delta\omega}{\omega} = 2.7 \times 10^{-3} (U^2 + V^2)^{1/2}$$

For a beam with no thermal spread, $(U^2 + V^2)$ is a function of two parameters, the frequency mismatch and the field in prebunching cavity S. The parameter S is proportional to the bunching parameter Q_b . The slow time scale code predicts frequency width as a function of bunching parameter Q_b for $m(\gamma\omega - \Omega)r_p / p\cos\alpha_e = 2$ as shown below:

Q_b	$\Delta\omega/\omega$
0.25	2×10^{-4}
0.5	4×10^{-4}
1.0	1.1×10^{-3}

In Fig. 5 is shown a contour plot of $(U^2 + V^2)^{1/2}$. Also shown are the positions of Q_b equal to 0.25, 0.5 and 1.0. Clearly, the analytic theory and the slow time scale code are in reasonable agreement for the low power, 85 GHz phase-locked oscillator experiment.

One of the most important things to quantify in designing the experiment is the mode conversion at the tapers, and equivalently, the cavity Q due to mode conversion. The mode conversion codes available to us did not account for standing modes in either the axial or azimuthal direction. Accordingly, these codes had to be modified to account for the actual mode structure. An example of the design is shown in Fig. 6. There, for a cavity with a straight section length of 0.19 cm, the Q due to mode conversion and the maximum magnetic field for oscillation (B_{∞}) are tabulated as a function of taper length. This latter quantity is calculated using the actual computed axial field profile, as it exists in the cavity and as it spills over into the drift section. There the minimum wall radius is 0.4 cm, and the maximum wall radius is 0.5 cm. Another important factor which contributes to the cavity Q is the slot angle of the cavity. This will be chosen to load down all the competing modes, but to allow the desired $TE_{1,1}$ mode to be excited, but not self oscillate. The cavity Q as a function of slot angle for the $TE_{1,1}$ (desired) and $TE_{0,1}$, and $TE_{2,1}$ (main competing) modes is shown in Fig. 7.

Since the input cavities have a large number of requirements regarding mode conversion, slot angle, mode excitation, and overall stability, we have minimized the risks by designing three different input cavities. These will be cold tested and

optimized on the actual experimental setup before it is pumped down. The coupling hole will be machined slightly too small, so that it can be easily enlarged. This cold test will determine the input cavity Q and the coupling from the EIO to the cavity. The coupling hole will be determined so as to optimally match the into the cavity. That is, the contribution to Q arising from the coupling hole will be equal to the contribution to Q from everything else. This will be cold tested on the three cavities. The wall radius, slot angle, effective length and predicted total Q for the three cavities are shown in Figs. 8a, b, and c. At optimal coupling, of course, the actual Q will be half of those values. Also shown are the computed axial field profiles. Notice that the effective length is not that strong a function of the physical length of the straight section of the cavity. The reason is that the evanescent region of the fields extend well into the drift section. Notice that the first cavity, the shortest one, has a very high predicted Q . This might appear incorrect because the large amount of mode conversion in the short taper would imply low Q . However, there is mode conversion at each taper, and it is possible that destructive interference between the forward converted $TE_{1,0}$ mode at the right taper and the backward converted $TE_{1,0}$ mode at the left taper could occur, thereby raising the Q . That is the basis of the design in Fig. 8a and the reason the predicted Q is so high. Whether this will actually work as predicted will be answered in the series of cold

tests. In Fig. 9a, b and c are shown the start oscillation currents of the three cavities for the $TE_{1,3}$ and $TE_{4,2}$ mode. Also shown is the start oscillation of the main oscillator cavities. Clearly there is a large range of currents where the input cavities will not oscillate at any value of magnetic field.

We now turn to the design of the main oscillator cavity. As this cavity will self oscillate at high power, it is particularly important that the mode conversion in the input taper be very small, so that it be isolated from the prebunching cavities. In Fig. 10 is shown the mode conversion from the $TE_{1,3}$ to $TE_{1,2}$ as a function of the input taper length. Also shown is the shift in the peak of the electric field profile. This shift essentially adds on to the physical separation of the two cavities. Since the mode conversion of the $TE_{1,2}$ back to $TE_{1,3}$ in the input cavities is always less than 15 dB (as quantified by the standard mode conversion codes for traveling waves) an input taper length of 0.4 cm will give at least 45 dB of isolation between two cavities. In Fig. III.11 are shown the wall radius, field amplitude and phase as a function of axial distance for the output cavity.

We now turn to some issues of the mechanical and electrical design of the low power phase-locked oscillator. A mechanical drawing of the experiment is shown in Fig. 11. Notice that the

input waveguide is pumped out in two places, at its entry to the tube, and also in a special pump out section near the input window. A preferable design would have been not to evacuate the input waveguide at all, but severe mechanical constraints prevent the use of a vacuum window inside the two inch bore of the superconducting magnet. Thus the only option is to put the input window outside of the magnet, and use an additional pumping port on the input waveguide. The electron gun to be used is the Varian VUW 8010 (Seftor) gun. This has been used in many experiments at NRL and is an extremely reliable piece of apparatus with which we have had a great deal of experience. Notice that after the gun, there is a space for the input and output cavity. For each, special cavity holders had to be designed, and the cavities themselves had to be designed to fit into them. The output cavity holder is the much more complicated and expensive holder, and the input cavity is the much more complicated and expensive cavity, for reasons we will go into shortly. There are also two current breaks, the first one, which is inside the magnet must be made of a nonmagnetic material; for the second, which is outside, can be either magnetic or nonmagnetic. The radiation leaves the tube through a beryllium oxide window.

We now turn to the input cavity. For all input cavities, the outside shape is the same, so the cavity holder is relatively

simple to design. The cavity itself is quite massive. The inside shape is machined to match the design of the inside wall which we have just discussed. Since the cavity is slotted, a thick piece of absorber must be used to absorb any microwave radiation coming out of the slot. This is a piece of ceralloy. Since the dielectric constant of the ceralloy is high, a matching piece of macor is used to eliminate reflections. This matching interface must be an odd number of quarter wavelengths thick. The frequency it is matched to is 92 GHz, the frequency of the $TE_{2,2}$ mode, the main competing mode. The bandwidth of the macor matching plate gets smaller as its thickness increases. For this reason, the most preferable thickness is one quarter wavelength. At this thickness, it will also be a good absorber for 85 GHz radiation; if the thickness is three quarters of a wavelength, there will be significant reflection there. However, machining such a thin, cylindrical piece of macor could be difficult, and it may be that we will have to settle for a thicker piece. A machine drawing of the input cavity is shown in Fig. 13.

The output cavity holder is one of the most complicated pieces to machine. To see this, note that there are three frequencies in the problem, the EIO frequency, the input cavity frequency, and the output cavity frequency. Clearly, one can only have a phase-locked oscillator if these three frequencies coincide to a very high degree of accuracy. The EIO is

mechanically tuneable over about 2 GHz. The input cavities are not designed to be tuneable, because the complications of hooking up the input microwaves would make a mechanical tuning scheme extremely complicated. Therefore the output cavity must be tuneable, so that all frequencies are tuned to the input cavity. To make the output cavity tuneable, we have utilized a slotted cavity design. A mechanical pusher compresses the cavity and slightly changes its shape and therefore its frequency (and cavity Q also). This plunger must be vacuum compatible. We have found that the mechanical design of the cavity which provides for reasonable amounts of compression (a few mills) with a reasonable force (a few pounds) is one in which the slots are brought all the way to the end of the cavity. Electrically, it is of course greatly preferable to bring the slots all the way to the narrow end of the cavity where there will be no microwave power. The output cavity holder then must be designed to transmit mechanical force through a vacuum enclosure. The actual transmitter will be a small bellows in the cavity holder which is machined separately from the rest of the cavity holder and welded on. A mechanical drawing of the cavity holder is shown in Fig. 14.

Notice that while the cavity is slotted, the main reason for the slots is not to provide mode control, but to allow for mechanical tuning. We have shown earlier that a $TE_{1,1}$ mode gyrotron at 70 kV can run with little mode competition in an unslotted cavity.² Thus, the output cavity holder has no

provision for using absorbers outside the slots. The actual output cavity, with slots and the axial tapers is three dimensional, and cannot be analyzed economically. What can be analyzed are two two dimensional approximations to it. First, we can use the slotted cavity code to calculate cavity frequency and Q as a function of slot width. The result of this calculation is shown in Fig. 15. Secondly, we can use the tapered cavity code (without slots) to calculate the frequency and Q as the cavity wall pivots about the end of the slots. The result of this calculation is also shown in Fig. 15. Clearly, compression of a few mills will give the sort of tuneability required, while not greatly affecting the Q. A machine drawing of the main oscillator cavity is shown in Fig. 16. Shown in Fig. 17 is a photograph of the input cavity holder, output cavity holder, and output cavity.

Finally, we turn to a discussion of the diagnostics of the low power phase-locked oscillator. Since this is a long pulse repeated experiment which will operate at high data rate, the diagnostics are simpler than in the single shot experiments which will be done at the megawatt and hundreds of megawatt level. A schematic of the diagnostic setup is shown in Fig. 18. The Varian EIO is launched through an isolator into the prebunching cavity of the gyrotron. The reflected power will be monitored. Another portion of the EIO signal will be branched off for

comparison with the gyrotron signal. The two signals are sent through variable attenuators so that the signals are of equal strength. They are then mixed in a balanced mixer, and the difference frequency signal is extracted. If the oscillator is phase-locked, then this signal will be a constant, which can be nulled by the use of a phase shifter in one of the lines. Another diagnostic line will sent the signal from both the EIO and gyrotron to a spectrum analyzer so as to to measure the spectrum of each in phase-locked as well as free running oscillation.

References

1. M. Rhinewine and M.E. Read, "A $TE_{1,3}$ Gyrotron at 85 GHz," Int. J. Electronics 61 (6), p. 729 (1986).
2. K.E. Kreisler and R.J. Temkin, "Single-Mode Operation of a High-Power, Step-Tunable Gyrotron," Phys. Rev. Lett. 59 (5), p. 547 (1987).
3. W.M. Manheimer, "Theory of the multi-cavity phase locked gyrotron oscillator," Int. J. Electronics 63 (1), p. 29 (1987).

IV. Febetron-Gyrotron Slotted Cavity Experiments

An experiment was carried out on the Febetron gyrotron facility to investigate $TE_{1,3}$ operation at 35 GHz through use of axial wall slots in the cavity to suppress competition with "whispering-gallery" modes. An earlier experiment produced 100 MW in a circularly-polarized $TE_{6,2}$ mode, and demonstrated frequency tuning over the range 28 to 49 GHz by operating in a family of $TE_{m,2}$ modes, with the azimuthal index "m" ranging from 4 to 10.¹ This experiment employed a 900 keV, 640 A electron beam, and successfully operated in the $TE_{1,3}$ mode at a power level of 35 MW, using a 2.34-cm-diameter cavity with a pair of opposing 45° axial wall slots. In the absence of slots, significant mode competition was observed from the $TE_{4,2}$ mode, so that stable operation in a circularly-polarized $TE_{1,3}$ mode was not possible. Through use of a cavity with 33° axial wall slots, it was possible to operate in a linearly-polarized $TE_{6,2}$ mode at ~48 GHz, while in the absence of slots it was straightforward to tune the interaction through the $TE_{4,2}$, $TE_{5,2}$, and $TE_{6,2}$ modes. These modes were observed through a gas breakdown technique, that permitted straightforward observation of the azimuthal index of the mode as well as the presence or absence of linear polarization. The results of this research have been accepted for publication in the IEEE Trans. Plasma Sci. A copy of the manuscript is attached as Appendix 5.

PHASE-LOCKED GYROKLYSTRON OSCILLATOR

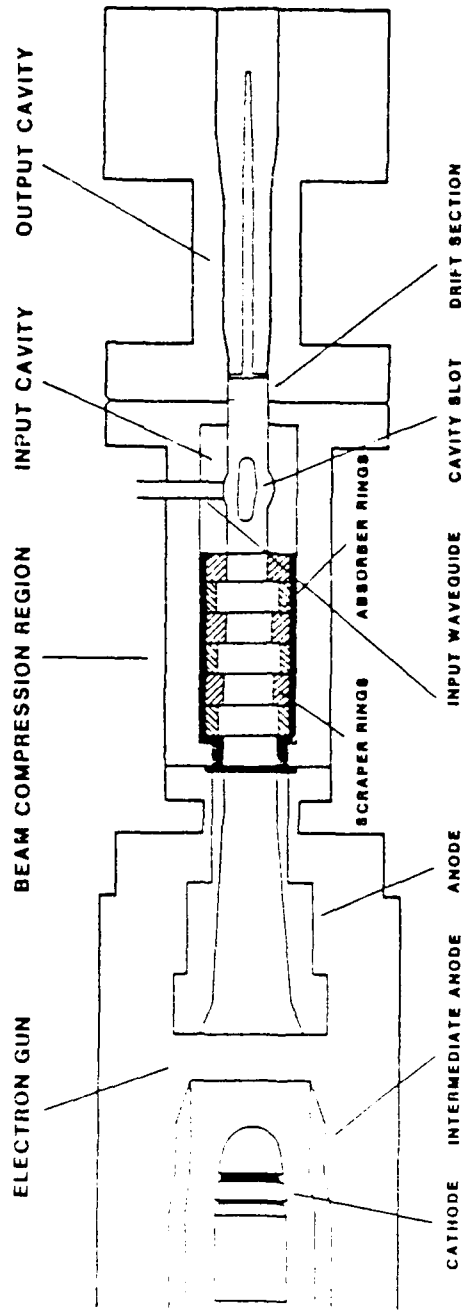
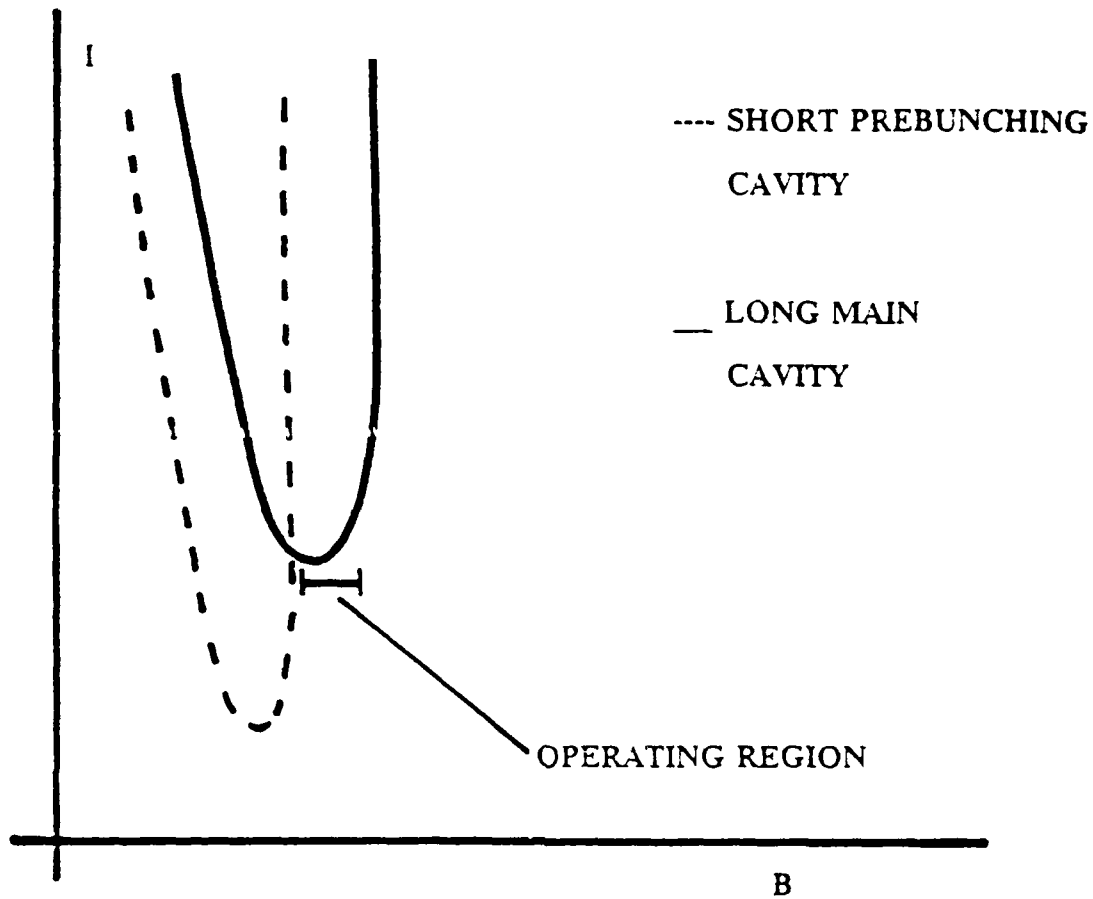


Fig. 1. Schematic of the low power experiment.

ORIGINAL I-B PARAMETER SPACE
FOR DOUBLE CAVITY PHASE LOCKED OSCILLATOR



- MAIN CAVITY OPERATES IN LOW EFFICIENCY REGION BECAUSE PREBUNCHING CAVITY HAS LOW THRESHOLD CURRENT BECAUSE OF ITS HIGH Q.
- GETTING A SIZEABLE PARAMETER WINDOW WHERE THE PREBUNCHING CAVITY IS STABLE PROVED VERY DIFFICULT.

Fig. 2. Original high Q input cavity design.

SINGLE CAVITY GYROTRON I-B
PARAMETER SPACE

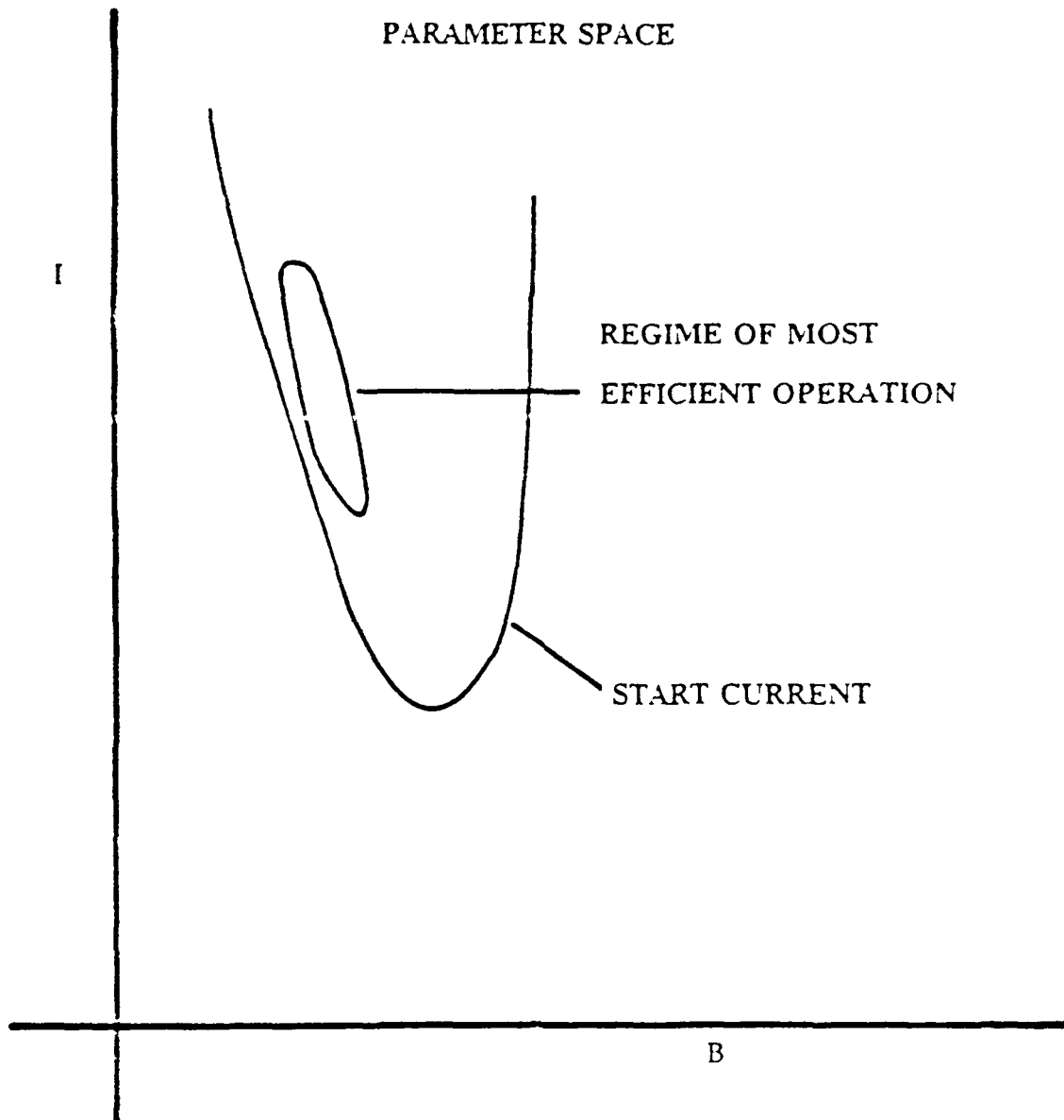
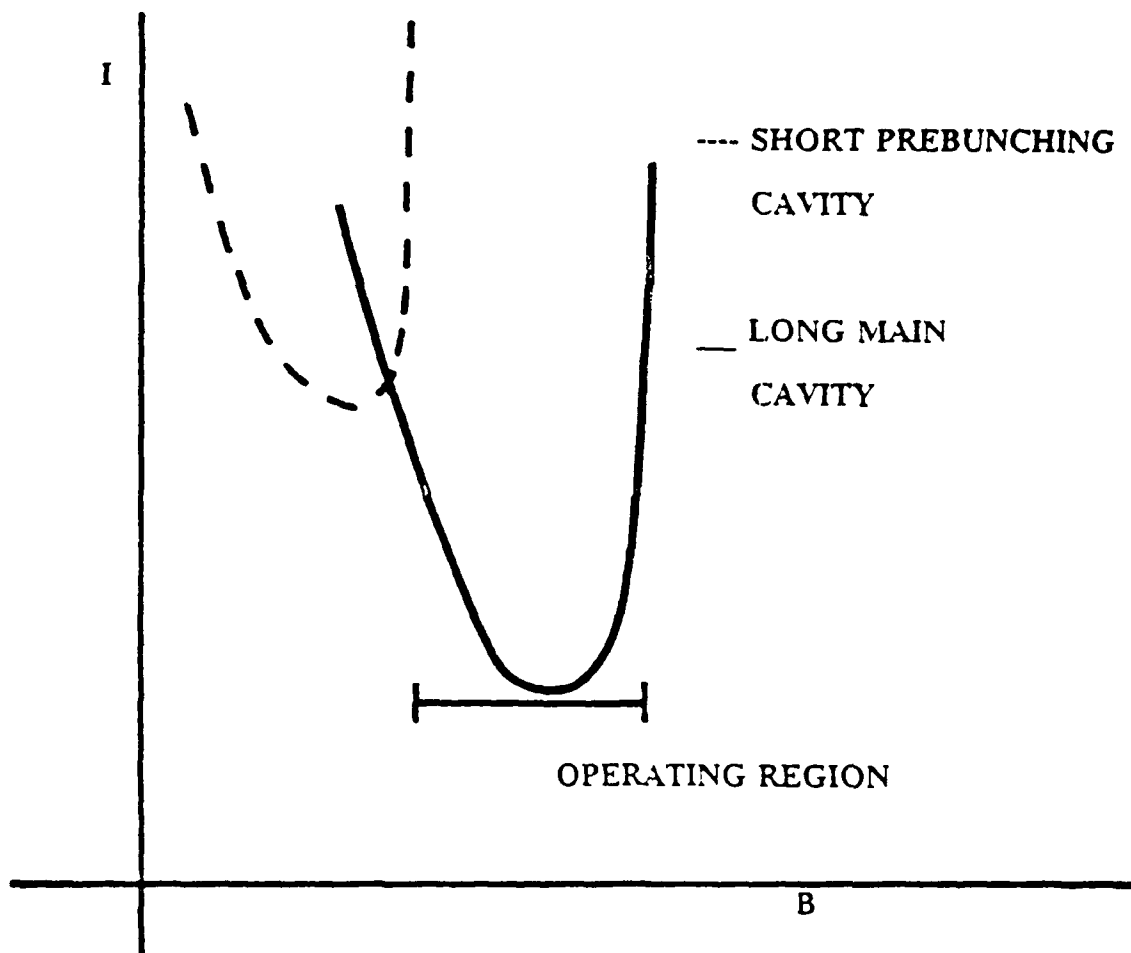


Fig. 3. Operating parameter space for a gyrotron.

I-B PARAMETER SPACE FOR DOUBLE CAVITY
REVISED DESIGN OF PHASE LOCKED OSCILLATOR



- OPERATING REGION NOW ENCOMPASSES HIGH EFFICIENCY OPERATION.
- CAN OPERATE BELOW MINIMUM START CURRENT OF PREBUNCHING CAVITY.
- INPUT FIELD CAN BE INCREASED BY GOING TO 3 CAVITIES. THIS SHOULD CONSIDERABLY INCREASE LOCKING BANDWIDTH.

Fig. 4. Revised low Q input cavity design.

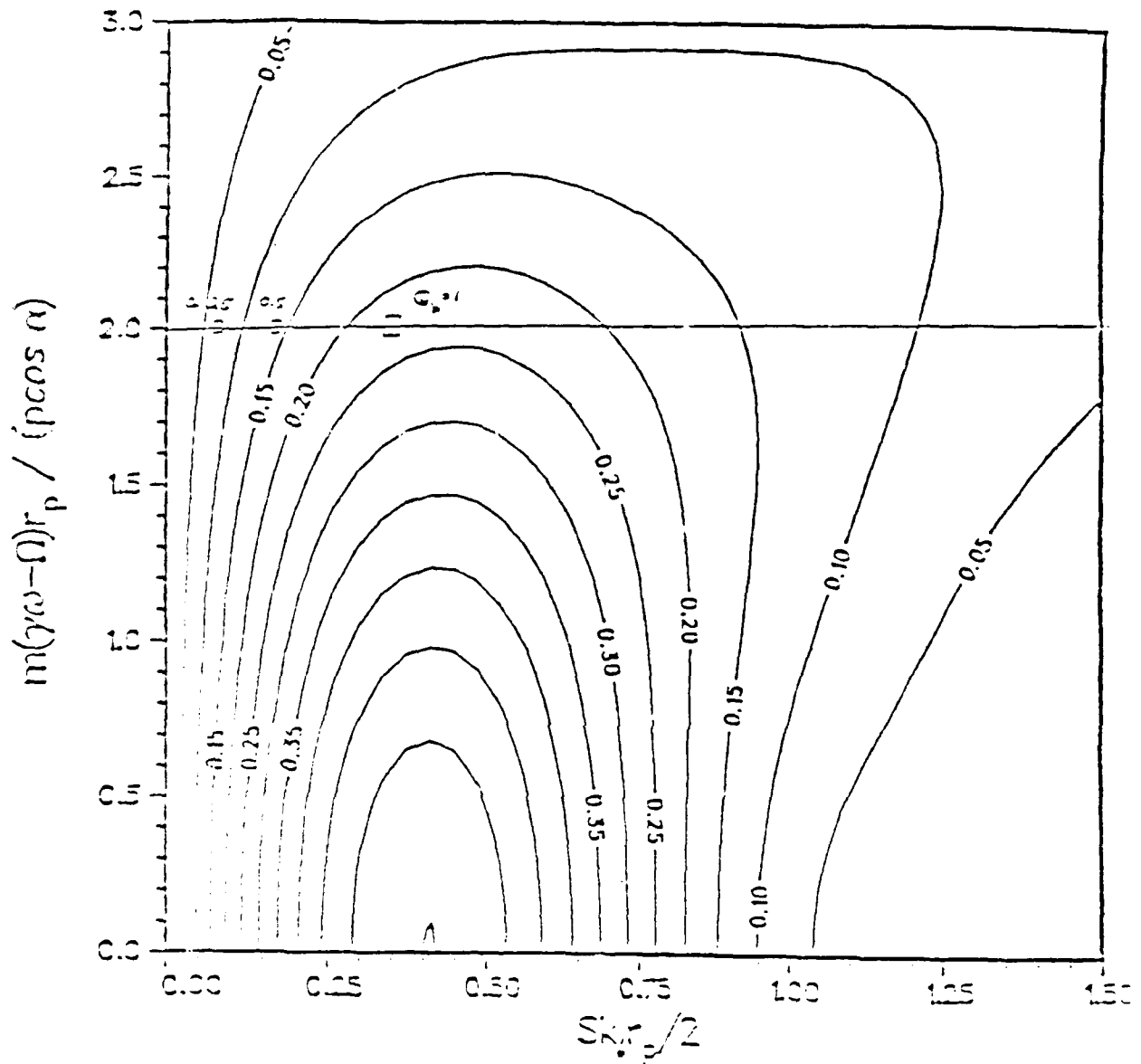


Fig. 3. Contours of $(U^2 + V^2)^{1/2}$. The values of $Q_p = 0.25$, 0.5 and 1.0 correspond to the values of S shown.

Cavity Q Due to Mode Conversion Losses and B_∞ versus Taper Length

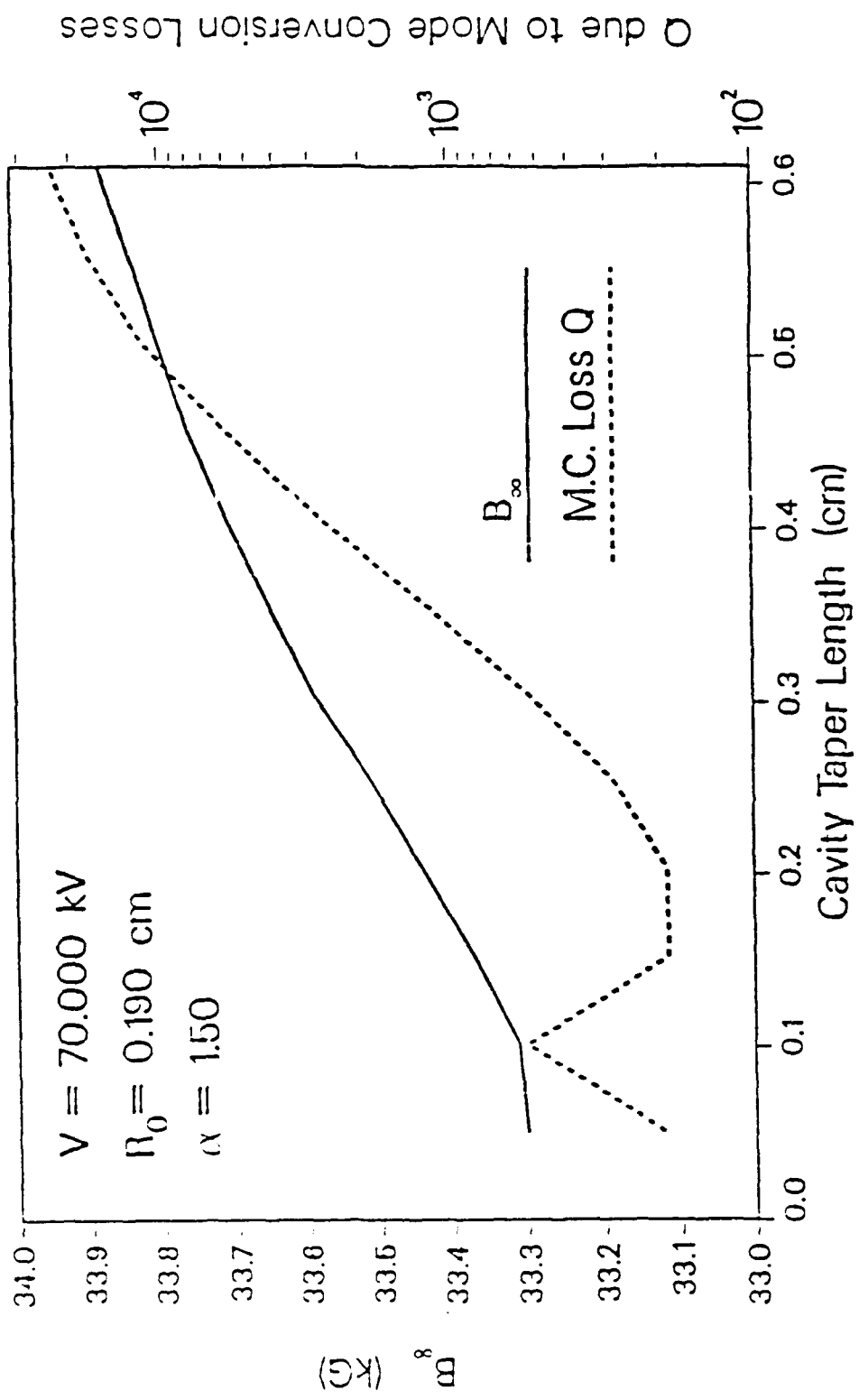


Fig. 6. Mode conversion and critical field as a function of taper length.

Mode Q versus Cavity Slot Full Angle

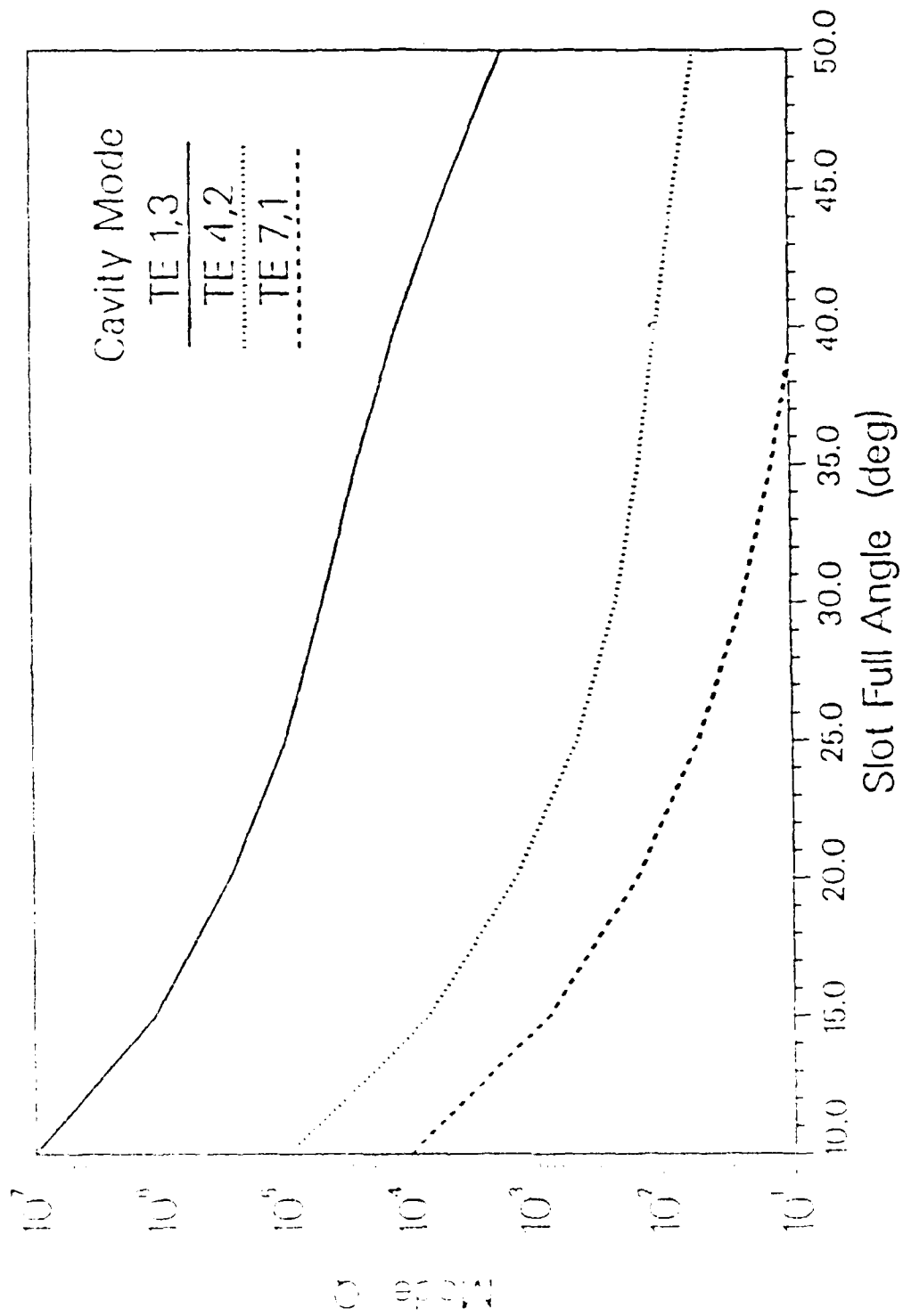


Fig. 7. Slotted cavity Q.

Longitudinal Field Function Amplitude versus Z

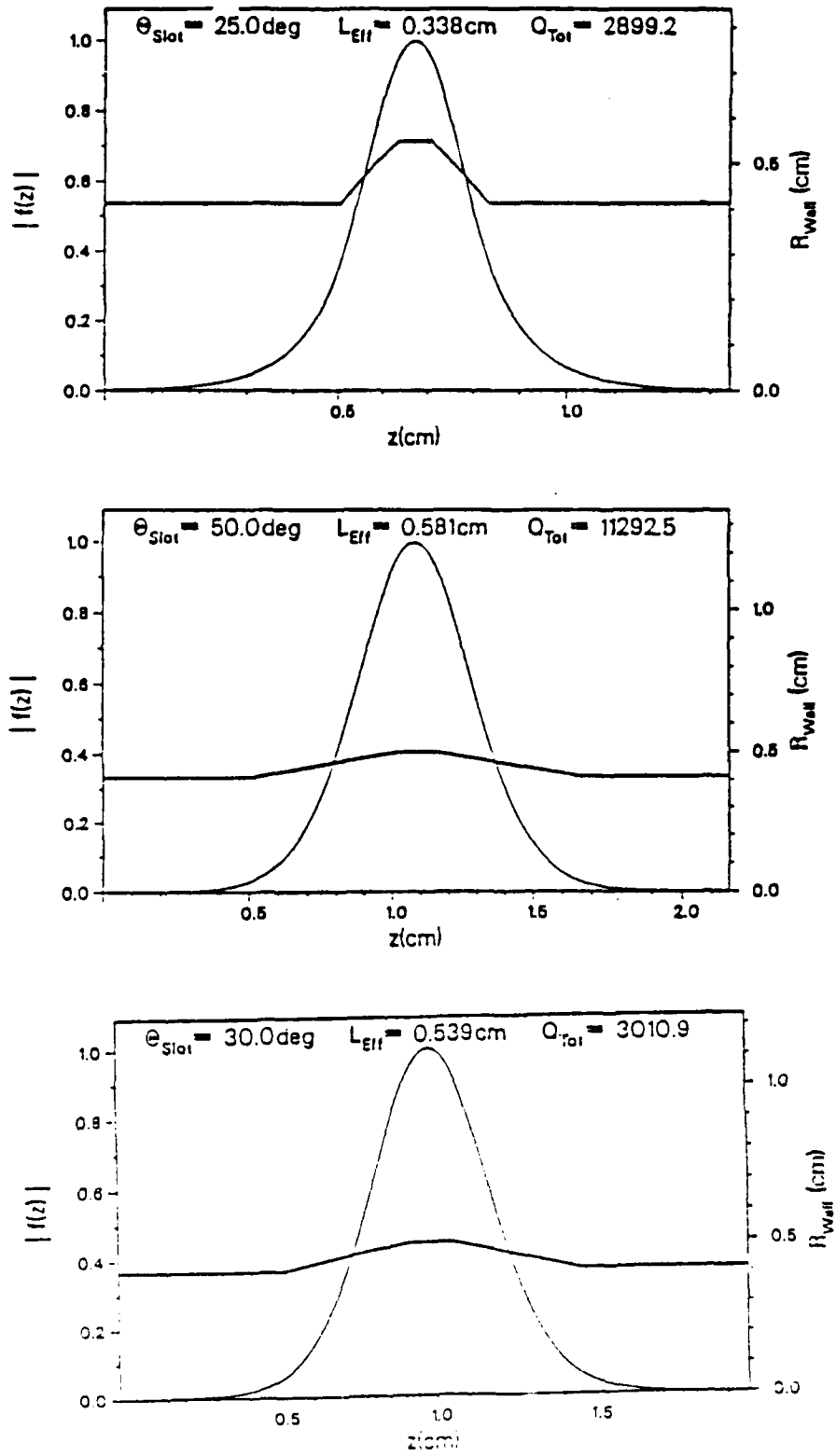


Fig. 8. The three input cavities.

Start Oscillation Current versus Magnetic Field

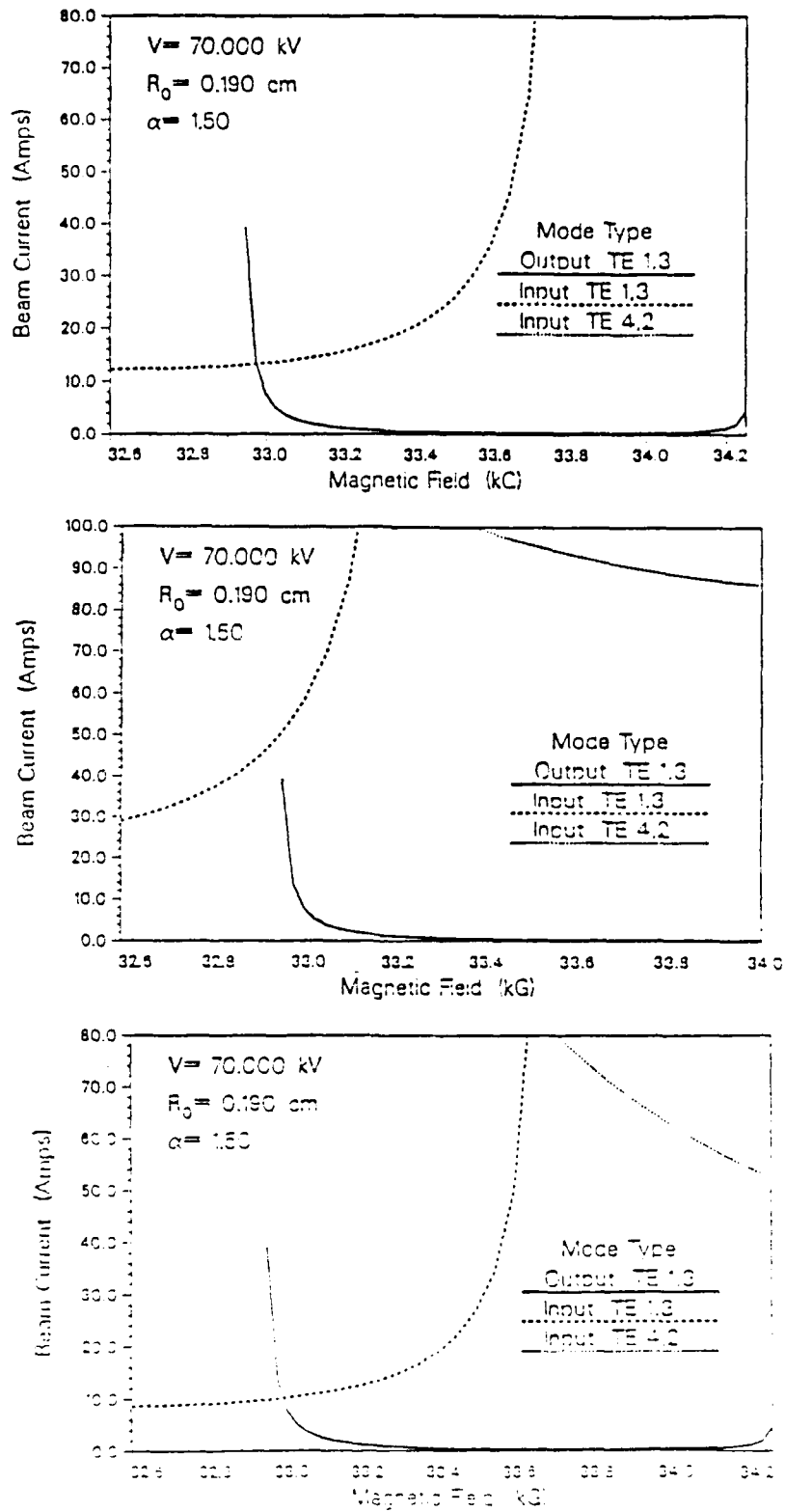


Fig. 9. Start currents for the input cavities.

Backward TE_{1,2} Mode Conversion and Profile Shift versus Cavity Taper Length

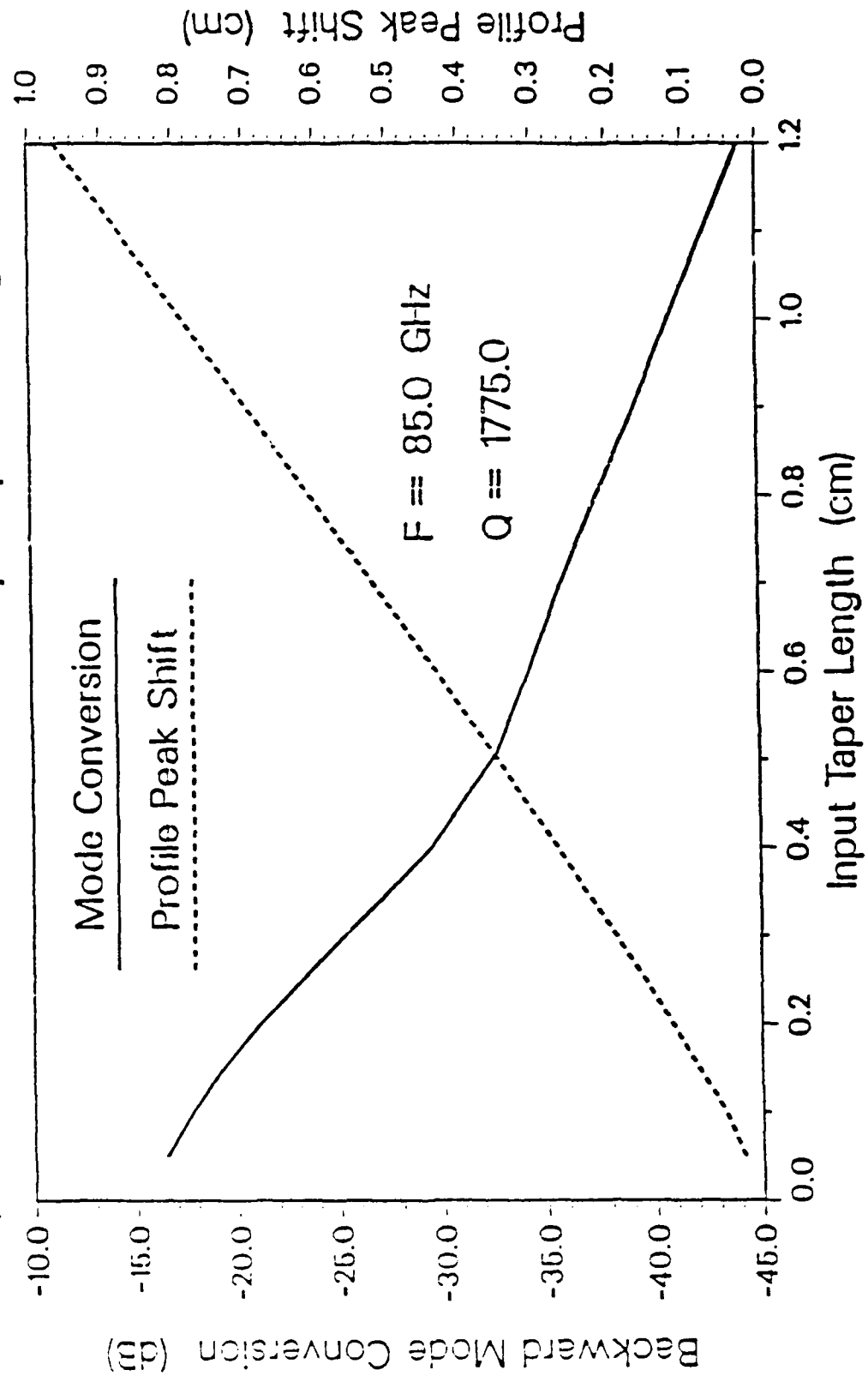


Fig. 10. Mode conversion in oscillator cavity.

Longitudinal Field Function Amplitude and Phase versus z

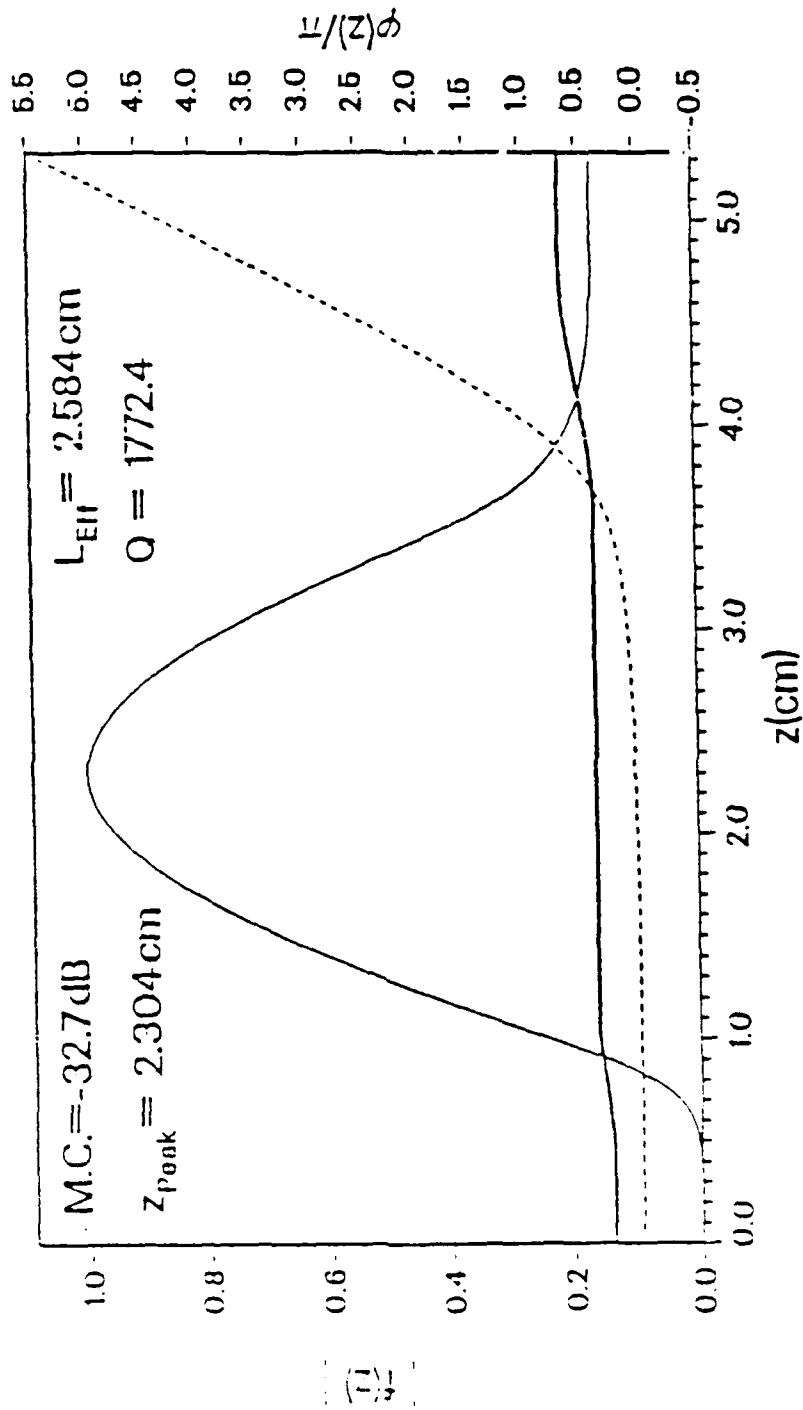


Fig. 11. The oscillator cavity.

TOP VIEW
85 GHz. PHASE-LOCKED GYROTRON
EXPERIMENTAL LAYOUT

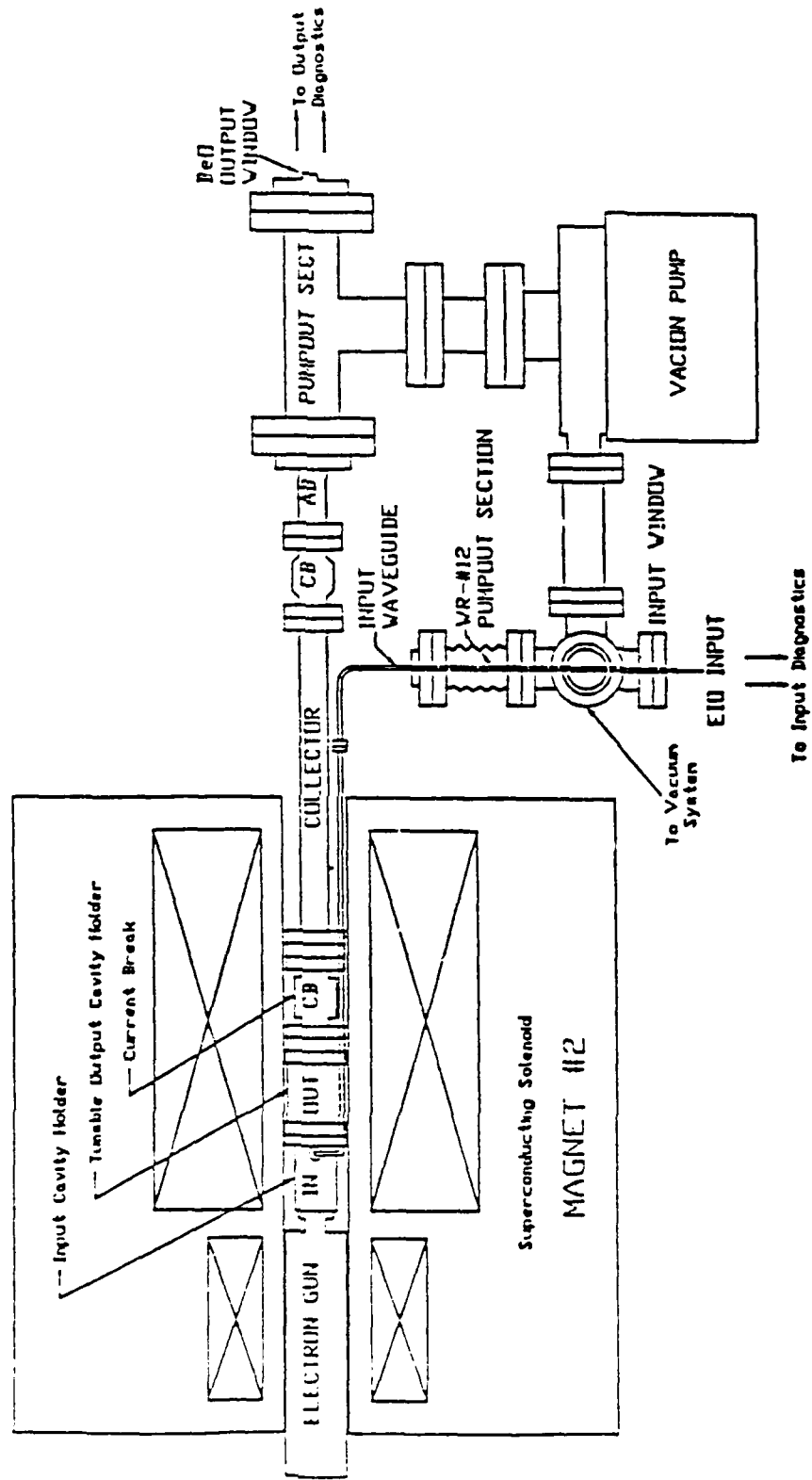


Fig. 12. Mechanical design of the low power phase-locked oscillator.

COPPER INPUT CAVITY

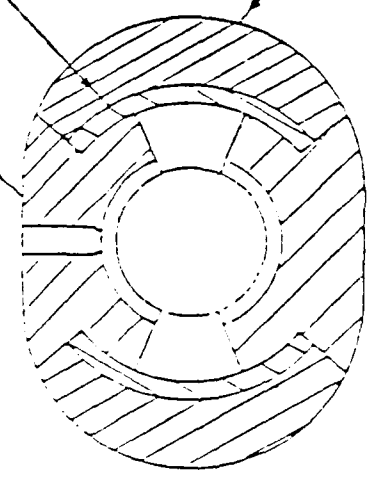
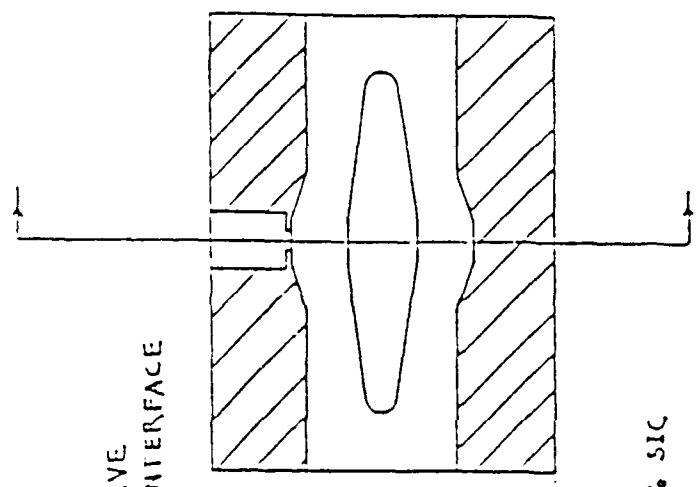
MACOR 1/4 WAVE
MATCHING INTERFACE

CERAMLOY

NO. 2710

60% BEO 40% SIC

ABSORBER



QTY. RECD.		QTY. RECD.		QTY. RECD.		QTY. RECD.		QTY. RECD.		QTY. RECD.	
-04		-03		-01		-01		-01		-01	
NOMENCLATURE OR DE											
ASSY. DASH NO.											

PARTS

Fig. 13. The input cavity.

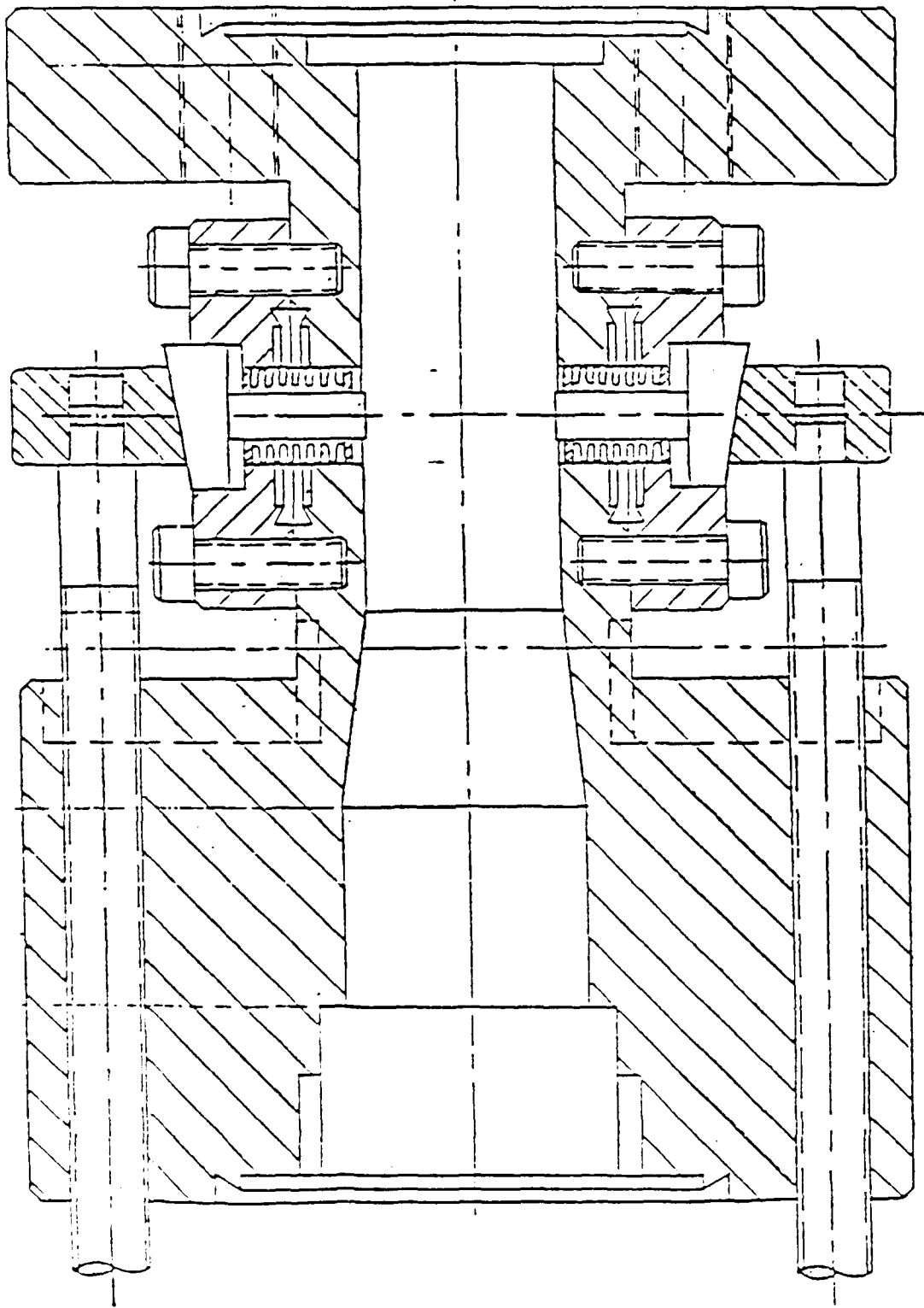


Fig. 14. The output cavity holder.

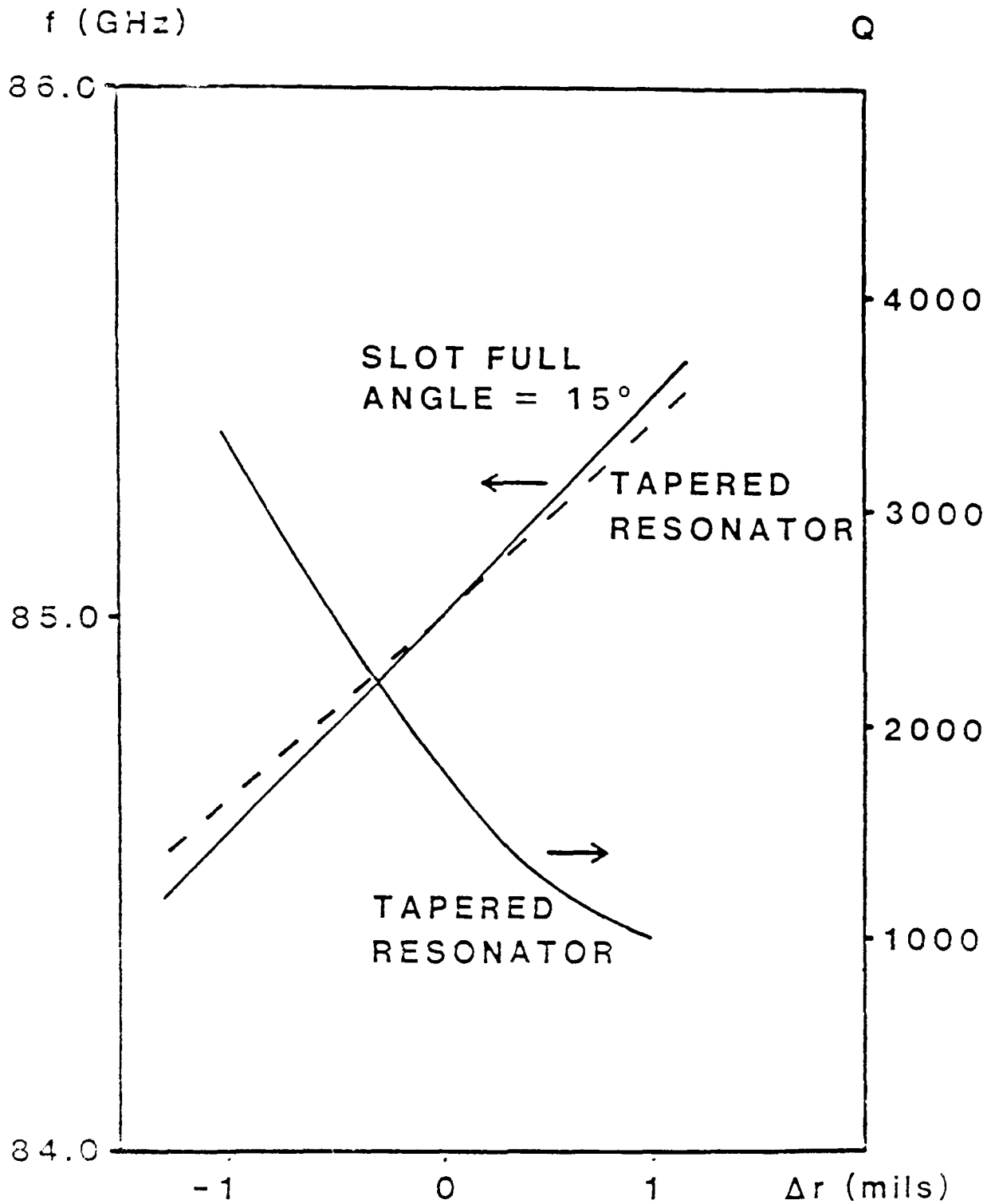


Fig. 15. Frequency as a function of slot width and taper displacement and cavity Q for the tapered cavity.

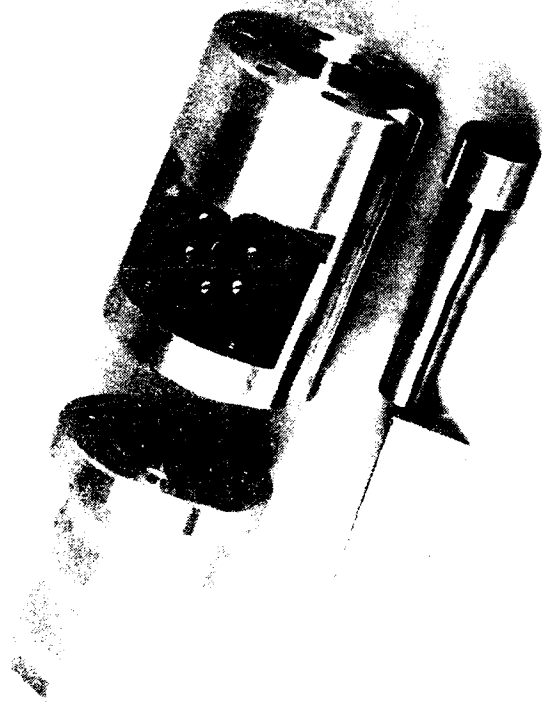


Fig. 17. The input and output cavity holder and the main cavity.

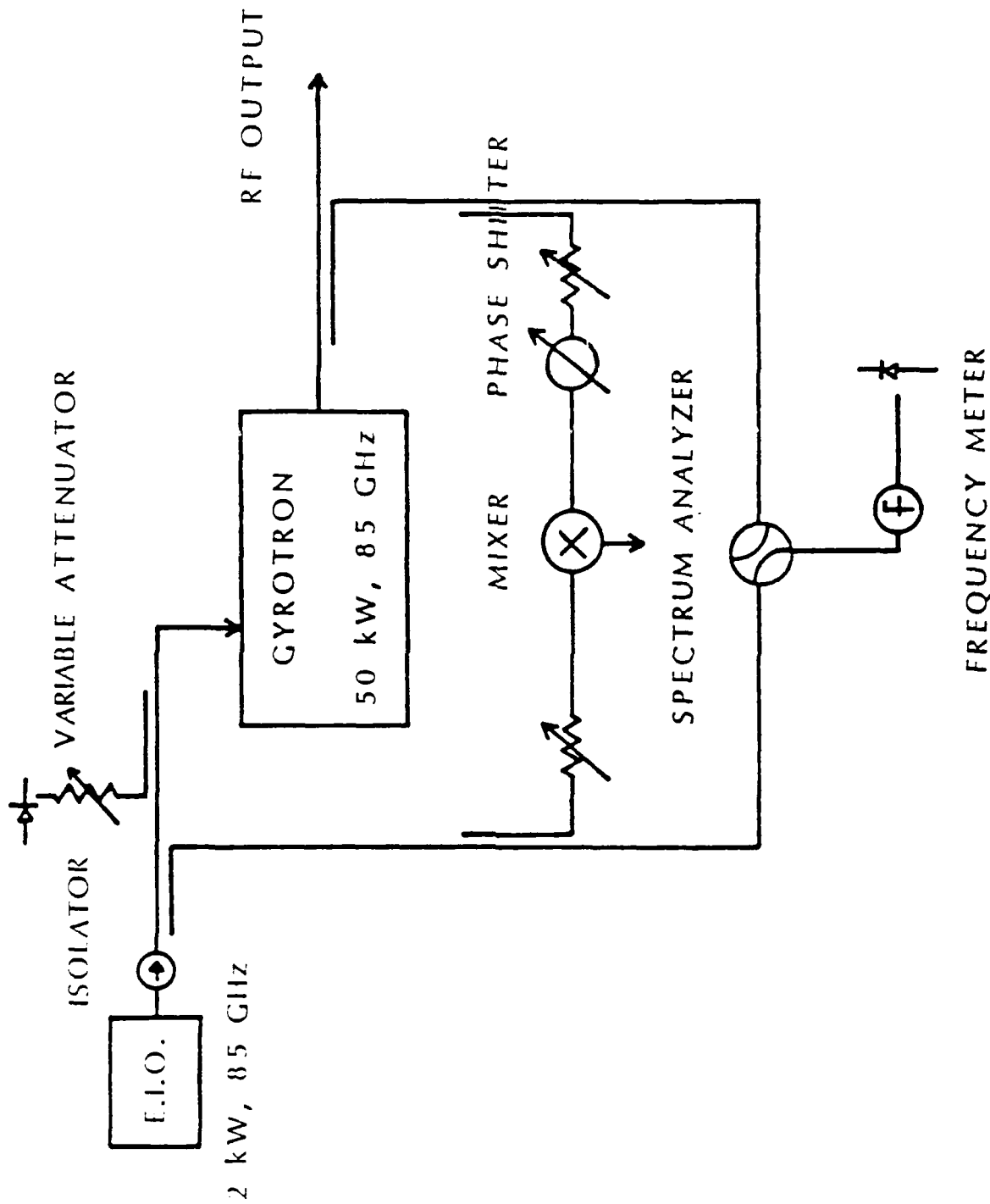


Fig. 18. Schematic of the diagnostic set up.

4740 DISTRIBUTION LIST

Air Force Avionics Laboratory
AFWAL/AADM-1
Wright/Patterson AFB, Ohio 45433
Attn: Walter Friez 1 copy

Air Force Office of
Scientific Research
Bolling AFB
Washington, D.C. 20332
Attn: H. Schlossberg 1 copy

Air Force Weapons Lab
Kirkland AFB
Albuquerque, New Mexico 87117
Attn: Dr. William Baker 2 copies
Dr. A.H. Guenter 1 copy

Columbia University
520 West 120th Street
Department of Electrical Engineering
New York, N.Y. 10027
Attn: Dr. S.P. Schlesinger 1 copy
A. Sen 1 copy

Columbia University
520 West 120th Street
Department of Applied Physics
and Nuclear Engineering
New York, New York 10027
Attn: T.C. Marshall 1 copy
R. Gross 1 copy

Cornell University
School of Applied and Engineering Physics
Ithica, New York 14853
Attn: Prof. Hans H. Fleischmann 1 copy
John Nation 1 copy
P. N. Sudan 1 copy

Creol-FEL Research Pavillion
12424 Research Parkway, Suite 400
Orlando, FL 32826
Attn: Dr. Luis R. Elias 1 copy
Dr. I. Kimel 1 copy

Dartmouth College
18 Wilder, Box 6107
Hanover, New Hampshire 03755
Attn: Dr. John E. Walsh 1 copy

Department of Energy Div. of Advanced Energy Projects Washington, DC 20545 Attn: Dr. R. Gajewski	1 copy
Department of Energy The Pentagon Washington, D.C. 20545 Attn: C. Finfgeld/ER-542, GTN T.V. George/ER-531, GTN D. Crandall/ER-55, GTN Dr. David F. Sutter/ER-224, GTN	1 copy 1 copy 1 copy 1 copy
Defense Advanced Research Project Agency/DEO 1400 Wilson Blvd. Arlington, Virginia 22209 Attn: Dr. S. Shey Dr. L. Buchanan	1 copy 1 copy
Defense Communications Agency Washington, D.C. 20305 Attn: Dr. Pravin C. Jain Assistant for Communications Technology	1 copy
Defense Nuclear Agency Washington, D.C. 20305 Attn: Mr. J. Farber Dr. Leon Wittwer (RAAE)	1 copy 5 copies
Defense Technical Information Center Cameron Station 5010 Duke Street Alexandria, Virginia 22314	2 copies
General Atomics 13-260 Box 85608 San Diego, CA 92138 ATTN: Dr. J. Doane Dr. C. Moeller	1 copy 1 copy
Georgia Tech. EES-EOD Baker Building Atlanta, Georgia 30332 Attn: Dr. James J. Gallagher	1 copy
Hanscomb Air Force Base Step 01, Massachusetts 01731 Attn: Lt. Rich Nielson ESD INF	1 copy

Hughes Aircraft Co.
Electron Dynamics Division
3100 West Lomita Boulevard
Torrance, California 90509
Attn: J. Christiansen 1 copy
J.J. Tancredi 1 copy

Hughes Research Laboratory
3011 Malibu Canyon Road
Malibu, CA 90265
Attn: Dr. R. Harvey 1 copy
Dr. R.W. Schumacher 1 copy

KMS Fusion, Inc.
3941 Research Park Dr.
P.O. Box 1567
Ann Arbor, Michigan 48106
Attn: S.B. Segall 1 copy

Lawrence Berkeley Laboratory
University of California
1 Cyclotron road
Berkeley, CA 94720
Attn: Dr. A.M. Sessler 1 copy

Lawrence Livermore National Laboratory
P.O. Box 808
Livermore, California 94550
Attn: Dr. D. Prosnitz 1 copy
Dr. T.J. Orzechowski 1 copy
Dr. J. Chase 1 copy
Dr. W.A. Barletta 1 copy
Dr. D.L. Birx 1 copy
Dr. R. Briggs 1 copy
Dr. E.T. Scharlemann 1 copy

Los Alamos National Scientific Laboratroy
P.O. Box 1663, MSJ 564
Los Alamos, NM 87545
Attn: Dr. Brian Newnam 1 copy

Los Alamos Scientific Laboratory
P.O. Box 1663, AT5-827
Los Alamos, New Mexico 87545
Attn: Dr. T.J.T. Kwan 1 copy
Dr. L. Thode 1 copy
Dr. C. Brau 1 copy
Dr. R. R. Bartsch 1 copy

Massachusetts Institute of Technology
 Department of Physics
 Cambridge, Massachusetts 02139
 Attn: Dr. G. Bekefi/36-213 1 copy
 Dr. M. Porkolab/NW 36-213 1 copy
 Dr. R. Davidson/NW 16-206 1 copy
 Dr. A. Bers/NW 38-260 1 copy
 Dr. K. Kreischer 1 copy
 Dr. B. Danby 1 copy
 Dr. G.L. Johnston 1 copy

Massachusetts Institute of Technology
 167 Albany St., N.W. 16-200
 Cambridge, Massachusetts 02139
 Attn: Dr. R. Temkin/NW 14-4107 1 copy

Spectra Technologies
 2755 Northup Way
 Bellevue, Washington 98004
 Attn: Dr. J.M. Slater 1 copy

Mission Research Corporation
 Suite 201
 5503 Cherokee Avenue
 Alexandria, Virginia 22312
 Attn: Dr. M. Bollen 1 copy
 Dr. Tom Hargreaves 1 copy
 Dr. J. Pasour 1 copy

Mission Research Corporation
 1720 Randolph Road, S.E.
 Albuquerque, New Mexico 87106
 Attn: Mr. Brendan B. Godfrey 1 copy

SPAWAR
 Washington, D.C. 20363
 Attn: E. Warden
 Code PDE 106-3113 1 copy
 Capt. Fontana
 PMW 145 1 copy

Naval Research Laboratory
 Addressee: Attn: Name/Code
 Code 1000 - Commanding Officer 1 copy
 Code 1001 - T. Coffey 1 copy
 Code 1200 - Capt M.A. Howard 1 copy
 Code 1220 - Security 1 copy
 Code 2628 - TID Distribution 22 copies
 Code 4000 - W. Ellis 1 copy
 Code 4000 - D. Nagel 1 copy
 Code 4700 - S. Ossakow 26 copies

Code 4700.1 - A.W. Ali	1 copy
Code 4710 - C. Kapetanakos	1 copy
Code 4740 - Branch Office	25 copies
Code 4740 - W. Black	1 copy
Code 4740 - A. Fliflet	1 copy
Code 4740 - S. Gold	1 copy
Code 4740 - A. Kinhead	1 copy
Code 4740 - W.M. Manheimer	1 copy
Code 4740 - M. Rhinewine	1 copy
Code 4770 - G. Cooperstein	1 copy
Code 4790 - B. Hui	1 copy
Code 4790 - C.M. Hui	1 copy
Code 4790 - Y.Y. Lau	1 copy
Code 4790 - P. Sprangle	1 copy
Code 5700 - L.A. Cosby	1 copy
Code 6840 - S.Y. Ahn	1 copy
Code 6840 - A. Ganguly	1 copy
Code 6840 - R.K. Parker	1 copy
Code 6840 - N.R. Vanderplaats	1 copy
Code 6850 - L.R. Whicker	1 copy
Code 6875 - R. Wagner	1 copy

Naval Sea Systems Command
 Department of the Navy
 Washington, D.C. 20362
 Attn: Commander
 PMS 405-300

1 copy

Northrop Corporation
 Defense Systems Division
 600 Hicks Rd.
 Rolling Meadows, Illinois 60008
 Attn: Dr. Gunter Dohler

1 copy

Oak Ridge National Laboratory
 P.O. Box Y
 Mail Stop 3
 Building 9201-2
 Oak Ridge, Tennessee 37830
 Attn: Dr. A. England

1 copy

Office of Naval Research
 800 N. Quincy Street
 Arlington, Va. 22217
 Attn: Dr. C. Roberson
 Dr. W. Condell
 Dr. T. Berlincourt

1 copy
 1 copy
 1 copy

Optical Sciences Center University of Arizona Tucson, Arizona 85721 Attn: Dr. Willis E. Lamb, Jr.	1 copy
Physics International 2700 Merced Street San Leandro, California 94577 Attn: Dr. J. Benford	1 copy
Physical Science Inc. 603 King Street Alexandria, VA 22314 ATTN: M. Read	1 copy
Princeton Plasma Plasma Physics Laboratory James Forrestal Campus P.O. Box 451 Princeton, New Jersey 08544 Attn: Dr. H. Hsuan Dr. D. Ignat Dr. H. Furth Dr. P. Efthimion Dr. F. Perkins	2 copies 1 copy 1 copy 1 copy 1 copy
Raytheon Company Microwave Power Tube Division Foundry Avenue Waltham, Massachusetts 02154 Attn: N. Dionne	1 copy
Sandia National Laboratories ORG. 1231, P.O. Box 5800 Albuquerque, New Mexico 87185 Attn: Dr. Thomas P. Wright Mr. J.E. Powell Dr. J. Hoffman Dr. W.P. Ballard Dr. C. Clark	1 copy 1 copy 1 copy 1 copy 1 copy
Science Applications, Inc. 1710 Goodridge Dr. McLean, Virginia 22102 Attn: Adam Drobot P. Vitello D. Bacon C. Menyuk	1 copy 1 copy 1 copy 1 copy
Science Research Laboratory 15 Ward Street Somerville, MA 02143 Attn: Dr. R. Shefer	1 copy

Stanford University Dept. of Electrical Engineering Stanford, CA 94305 Attn: Dr. J. Feinstein	1 copy
Stanford University High Energy Physics Laboratory Stanford, California 94305 Attn: Dr. T.I. Smith	1 copy
Stanford University SLAC Stanford, CA 94305 Attn: Dr. Jean Labacqz	1 copy
TRW, Inc. One Space Park Redondo Beach, California 90278 Attn: Dr. H. Boehmer Dr. T. Romisser Dr. Z. Guiragossian	1 copy 1 copy 1 copy
University of California Physics Department Irvine, California 92717 Attn: Dr. G. Benford Dr. N. Rostoker	1 copy 1 copy
University of California Department of Physics Los Angeles, CA 90024 Attn: Dr. A.T. Lin Dr. N. Luhmann Dr. D. McDermott	1 copy 1 copy 1 copy
University of Maryland Department of Electrical Engineering College Park, Maryland 20742 Attn: Dr. V. L. Granatstein Dr. W. W. Destler	1 copy 1 copy
University of Maryland Laboratory for Plasma and Fusion Energy Studies College Park, Maryland 20742 Attn: Dr. Tom Antonsen Dr. John Finn Dr. Jhan Varyan Hellman Dr. W. Lawson Dr. Baruch Levush Dr. Edward Ott Dr. M. Reiser	1 copy 1 copy 1 copy 1 copy 1 copy 1 copy 1 copy

University of Tennessee Dept. of Electrical Engr. Knoxville, Tennessee 37916 Attn: Dr. I. Alexeff	1 copy
University of New Mexico Department of Physics and Astronomy 800 Yale Blvd, N.E. Albuquerque, New Mexico 87131 Attn: Dr. Gerald T. Moore	1 copy
University of Utah Department of Electrical Engineering 3053 Merrill Engineering Bldg. Salt Lake City, Utah 84112 Attn: Dr. Larry Barnett Dr. J. Mark Baird	1 copy 1 copy
Director of Research U. S. Naval Academy Annapolis, Maryland 21402-5021	1 copy
U. S. Army Harry Diamond Labs 2800 Powder Mill Road Adelphi, Maryland 20783-1145 Attn: Dr. Howard Brandt Dr. Edward Brown Dr. Stuart Graybill Dr. A. Kehs Dr. J. Silverstein	1 copy 1 copy 1 copy 1 copy 1 copy
Varian Associates 611 Hansen Way Palo Alto, California 94303 Attn: Dr. H. Huey Dr. H. Jory Dr. Kevin Felch Dr. R. Pendleton Dr. A. Salop	1 copy 1 copy 1 copy 1 copy 1 copy
Varian Eimac San Carlos Division 301 Industrial Way San Carlos, California 94070 Attn: C. Marshall Loring	1 copy
Yale University Applied Physics Madison Lab P.O. Box 2159 Yale Station New Haven, Connecticut 06520 Attn: Dr. I. Bernstein	1 copy

END

FILMED

6-89

DTIC